

An Efficient Method for the Production of Isotopically Enriched Cholesterol for NMR

Rupali Shivapurkar, Cleiton M. Souza, Damien Jeannerat and Howard Riezman

Supplementary Data

Mass spectra of the enriched cholesterol samples; description of the algorithm used for the calculations of the mass spectra and the NMR multiplicities; discussion of the influence of the enrichment levels of (u - $^{13}\text{C}_6$) glucose, (1 - $^{13}\text{C}_1$) glucose and (2 - $^{13}\text{C}_1$) glucose on the isotopomer distributions of cholesterol; simulations of the proportions of multiplet structures as a function of the enrichment level of cholesterol; Table of J_{CC} calculated by DFT/GIAO methods.

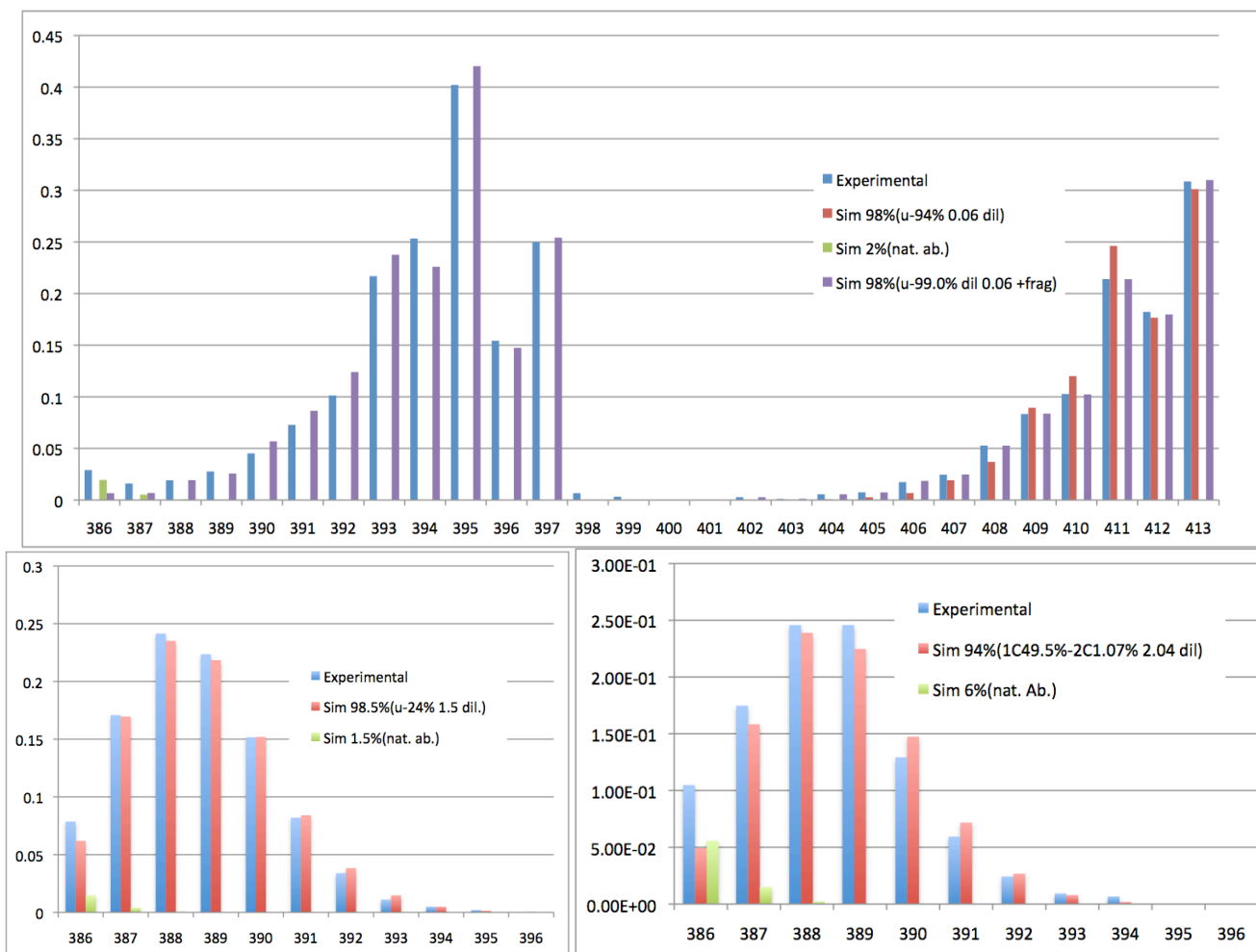


Figure S1. Experimental (blue) and simulated (red, green and purple) MS spectra of cholesterol produced with ($u\text{-}^{13}\text{C}_6$, 99%) glucose (top) 2:3 ($u\text{-}^{13}\text{C}_6$, 24%)/($u\text{-}^{13}\text{C}_6$, 1.07%) glucose (bottom left), and 1:2 ($^{13}\text{C}_1$, 99%)/($u\text{-}^{13}\text{C}_6$, 1.07%) glucose (bottom right). The simulated spectra were calculated using a simplified version of the method proposed by Kelleher *et al.*⁵ (see below). The enrichment levels were set according to the values certified by the producer. For the top figure, where the enriched glucose was not diluted with natural abundance glucose, the small dilutions due to the yeast extract was determined to be equal to 2%. For the others, the simulations match the experimental data with the values calculated based on the quantity of added natural-abundance glucose. (purple) The fragmentation corresponding to the loss of a $^{13}\text{CH}_3$ [MM-16] and H_2O [MM-18] were included in the calculations. The proportions of natural abundance cholesterol (in green) were estimated based on the difference of 386 signals in experimental and the simulated spectra.

Simulations of the mass spectra and the distributions of and the NMR multiplicities

The distribution of isotopomers were calculated on a desktop PC using a C program taking the ^{13}C abundance for the two type of carbons (see Fig. 1) e_1 (empty circles in Figure 1) and e_2 (filled circles in Figure 1) and a factor of dilution d as input and summing the probabilities of the 2^{27} isotopomers according to their masses or the multiplicities of a specific carbon. The probability p^{tot} of a given isotopomer is

$$p^{tot} = \prod p_i \cdot \prod q_j \cdot \prod r_k$$

where p_i are the probability of the isolated carbons $i = 1, 15, 22, 26$ to be enriched or not:

$$p_i = (e_i + 0.0107 \cdot d) / (1 + d) \text{ when the carbon } i \text{ is enriched}$$

$$p_i = ((1 - e_i) + (1 - 0.0107) d) / (1 + d) \text{ when the carbon } i \text{ is not enriched,}$$

q_j is the probability of the isolated carbon $j = 4$ to be enriched or not:

$$q_j = (e_2 + 0.0107 \cdot d) / (1 + d) \text{ when the carbon } j \text{ is enriched,}$$

$$q_j = ((1 - e_2) + (1 - 0.0107) d) / (1 + d) \text{ when the carbon } j \text{ is not enriched,}$$

and r_k , are the probabilities for the 11 pairs of carbons $k = 3, 5, 7, 9, 13, 17, 18, 19, 21, 24, 27$ and their partners stemming from the same acetyl CoA (rounded frames in Fig. 1) to be in any of the four possible enrichment patterns:

$$r_k = (e_1 \cdot e_2 + 0.0107^2 \cdot d) / (1 + d) \text{ when the carbon } k \text{ and its partner are enriched,}$$

$$r_k = (e_1(1 - e_2) + 0.0107(1 - 0.0107) \cdot d) / (1 + d) \text{ when the carbon } k \text{ is enriched but its partner is not,}$$

$$r_k = ((1 - e_1) e_2 + (1 - 0.0107)0.0107 \cdot d) / (1 + d) \text{ when the carbon } k \text{ is not enriched but its partner is,}$$

$$r_k = ((1 - e_1)(1 - e_2) + (1 - 0.0107)^2 \cdot d) / (1 + d) \text{ when neither the carbon } k \text{ nor its partner is enriched.}$$

The multiplicities are determined according to the number of coupling partners a given carbon has with J_{CC} exceeding a user-defined threshold. The coupling constants considered in the calculations can be found in Table S1 while the thresholds are given in the figure legends.

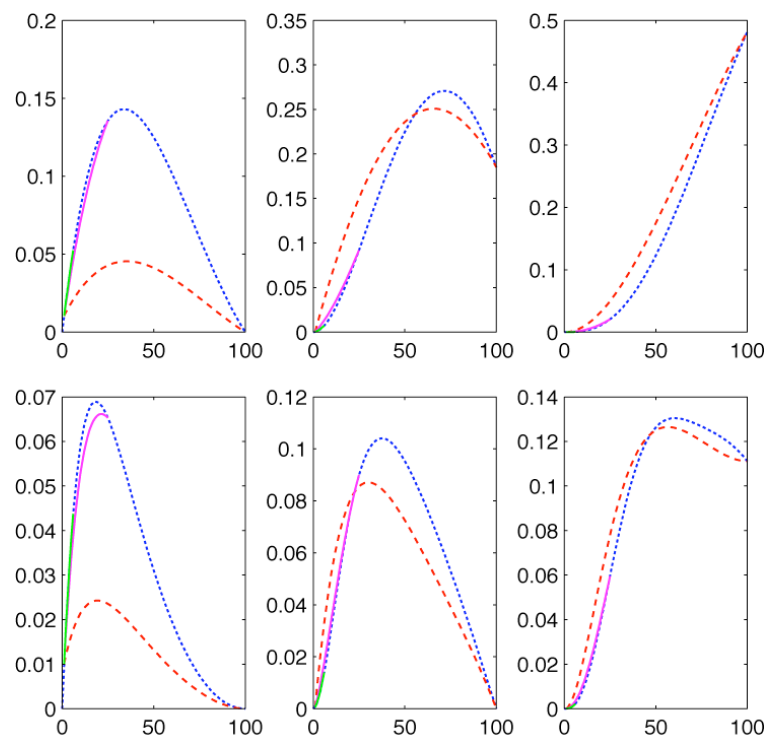


Figure S2. Simulations of the proportions of singlet (left), doublet (center) and triplet (right) structures as a function of the enrichment level of cholesterol. The criterion to consider couplings was ${}^1J_{CC}$ (top) and ${}^1J_{CC} > 1$ Hz (bottom). The sources of glucose were ($u\text{-}^{13}\text{C}_6$, $e\%$) (blue), diluted commercially available ($u\text{-}^{13}\text{C}_6$, 100%) (red) ($u\text{-}^{13}\text{C}_6$, 25%) (magenta) and ($u\text{-}^{13}\text{C}_6$, 6%) (green). For the singlets, the blue line reaches 0.14 for 33.8% enrichment and the red line 0.045 for 35.3% enrichment for ${}^1J_{CC}$ and 0.69 for 18.4% respectively 0.02 for 19.3% when considering $J_{CC} > 1$ Hz.

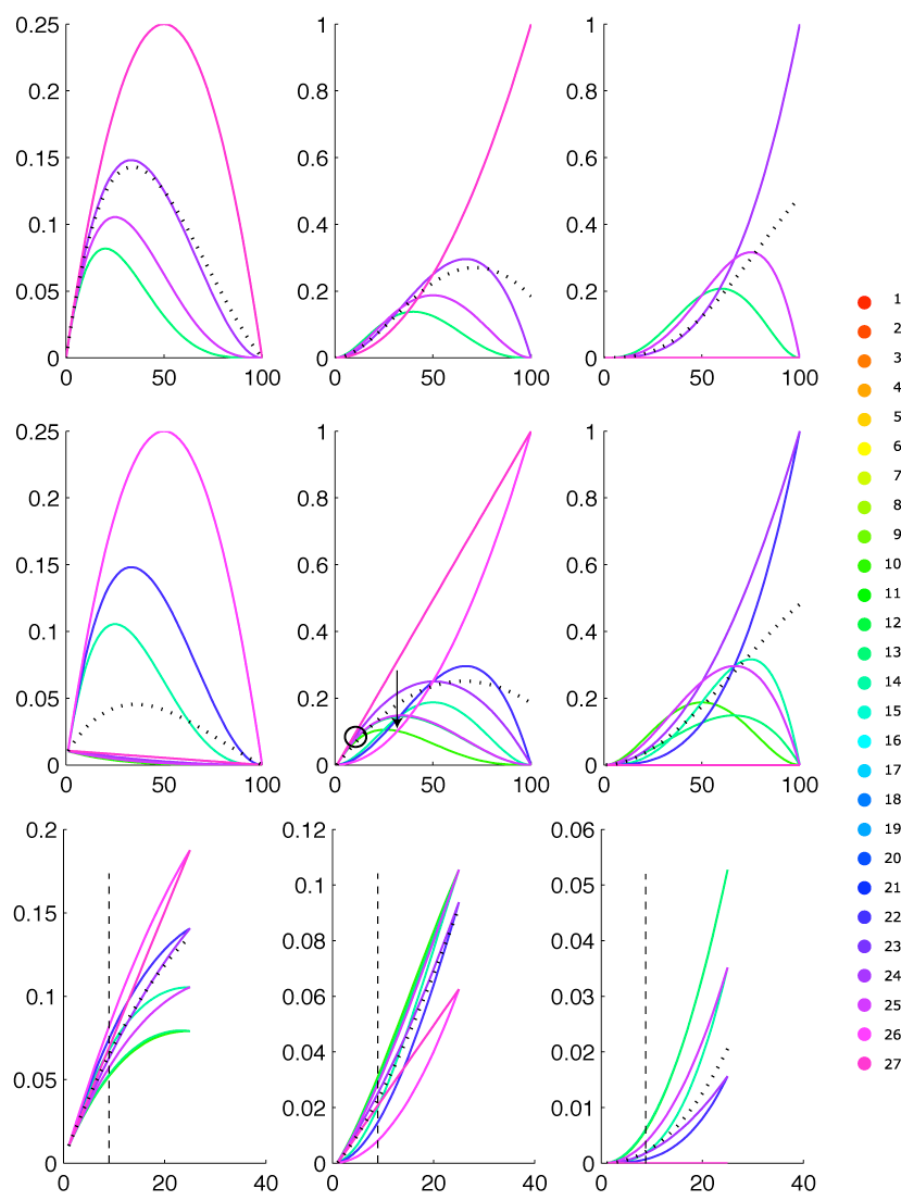


Figure S3. Simulations of the proportions of singlet (left), doublet (center) and triplet (right) structures for $J_{CC} > 25$ Hz (only $^1J_{CC}$) as a function of the level of ^{13}C enrichment of cholesterol. The sources of glucose were ($u\text{-}^{13}\text{C}_6\text{-glucose}$, $e\%$) (top), diluted ($u\text{-}^{13}\text{C}_6\text{-glucose}$, 100%) (middle) and diluted ($u\text{-}^{13}\text{C}_6\text{-glucose}$, 24%) (bottom). The dotted curves correspond to the average of the others. The vertical dotted lines indicate the conditions used for the preparation of the 9.49% enriched cholesterol illustrated in Figure 1 B.

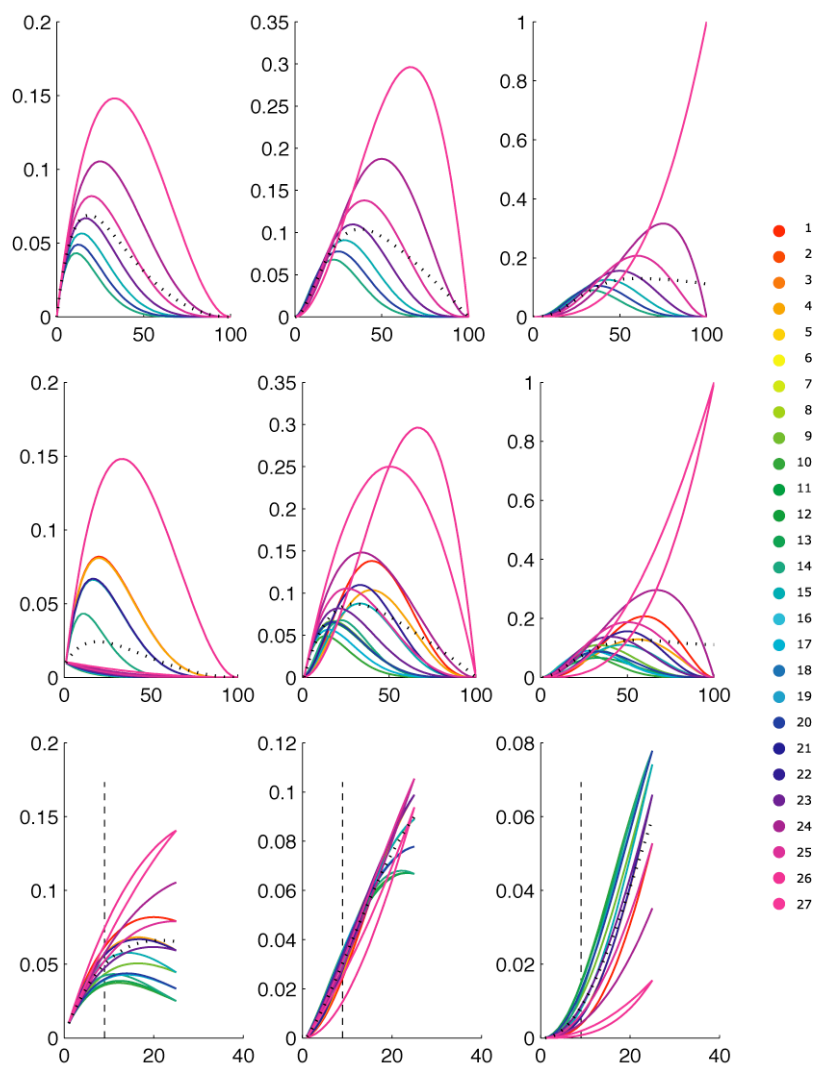


Figure S4. Simulations of the proportions of singlet (left), doublet (center) and triplet (right) structures for $J_{CC} > 1$ Hz as a function of the level of ^{13}C enrichment of cholesterol. The sources of glucose were ($u\text{-}^{13}\text{C}_6$, e%) glucose (top), diluted ($u\text{-}^{13}\text{C}_6$, 100%) glucose (middle) and diluted ($u\text{-}^{13}\text{C}_6$, 24%) glucose (bottom). The dotted curves correspond to the average of the others. The vertical dotted lines indicate the conditions used for the preparation of the 9.49% enriched cholesterol illustrated in Figure 1B.

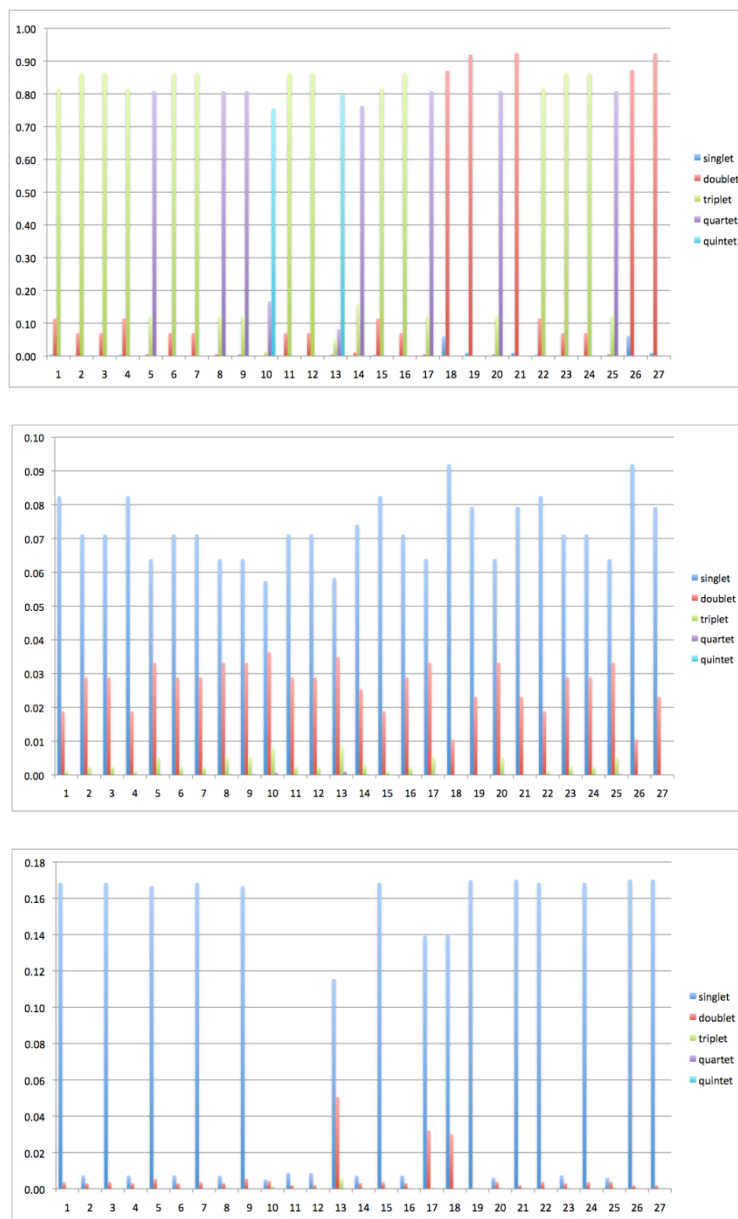


Figure S5. Simulations of the distributions of the $^1J_{CC}$ multiplicities of cholesterol obtained from (u - $^{13}C_6$, 99%) glucose (top) 2:3 (u - $^{13}C_6$, 24%)/(u - $^{13}C_6$, 1.07%) glucose (middle), and 1:2 (1 - $^{13}C_1$, 99%)/(u - $^{13}C_6$, 1.07%) glucose (bottom).

Influence of the enrichment levels of (u - $^{13}\text{C}_6$) glucose on the isotopomer distribution of cholesterol

Diluting n times (u - $^{13}\text{C}_6$, 100%) 2:3 with natural-abundance glucose to obtain a given percentage e of enrichment does not result in the same distribution of isotopomers as directly using (u - $^{13}\text{C}_6$, $e\%$) glucose. For most pairs of carbons, the probability for the neighboring carbons of a ^{13}C to be enriched is close to $e/(n+1)\%$ (when e is larger than 1.07%, the ^{13}C natural abundance), but if the carbon-13 is in one of the rounded frames of Figure 1, the probability for the neighbor to be ^{13}C is $e\%$ because both carbons originate from the same glucose molecule. Comparing curves of Figure S2 shows that the average proportion of singlet reaches an average intensity of 14.3% with 33.84% enrichment when considering only $^1J_{\text{CC}}$, and 6.9% at 18.4% enrichment for $J_{\text{CC}} > 1$ Hz. In practice, one may not have glucose sources for these enrichment levels and may need to dilute commercially available sources (100, 25 and 6% for uniform enrichments). For HSQC-based experiments (u - $^{13}\text{C}_6$, 98-99%) glucose is not a good source because singlets would account for only one third of the maximum level (compare the red and the blue lines in Figure S2 left). On the other hand, dilution of the commercially available (u - $^{13}\text{C}_6$, 25%) glucose results in isotopomer distributions close to the level of (u - $^{13}\text{C}_6$, $e\%$) as the magenta and blue lines almost overlap in Figure S2 left. This observation is also valid when considering all J_{CC} larger than 1 Hz. (Figure S2 bottom). The conclusion is that uniformly labeled glucose cannot provide more than *c.a.* 7-15% singlet. One should turn to finer, but also more expensive sources of enriched glucose like (1 - $^{13}\text{C}_1$), (2 - $^{13}\text{C}_1$) or, even better, (1 , 6 - $^{13}\text{C}_2$), (2 , 5 - $^{13}\text{C}_2$) glucose to overcome this limitation (see below).

When considering the production of cholesterol for double-quantum experiments (based on pairs of ^{13}C , i.e. doublets in carbon spectra), (u - $^{13}\text{C}_6$, 98-99%) glucose is a very good source of ^{13}C . The relative proportion of the doublets can reach about 25% when considering only $^1J_{\text{CC}}$ and 10% when taking into account all $J_{\text{CC}} > 1$ Hz (See Figures S2-S4). This is quite high compared to the 0.01% natural abundance but very uneven depending on the environment of each carbon. It may be better to target 32% average

enrichment (see the position of the arrow in Figure S3) using ($u\text{-}^{13}\text{C}_6$, 99%)/($u\text{-}^{13}\text{C}_6$, 1.07%) glucose 1:2. Under these conditions, all the carbons should have at least 10% of the maximal signal amplitude with an average of 18.2%. A more economical alternative is to prepare 10% average enrichment (circle in Figure S3) using ($u\text{-}^{13}\text{C}_6$, 99%)/($u\text{-}^{13}\text{C}_6$, 1.07%) glucose 1:8.5. This should provide approximately 7% of the maximal signal amplitude for all the pairs of carbons in the rounded frames of Figure 1.

Distribution of the carbon multiplicity of enriched cholesterol produced using diluted ($1\text{-}^{13}\text{C}_1$, 99%) and ($2\text{-}^{13}\text{C}_1$, 99%) glucose

Simulations of the multiplicity distribution of signals of glucose produced using ($1\text{-}^{13}\text{C}_1$, 99%) glucose (Figure S6) and ($2\text{-}^{13}\text{C}_1$, 99%) glucose (Figure S7) show that most carbons have the ideal linear relationship between enrichment level and signal intensity thanks to the absence of direct coupling partners. Only the curves for carbons 13, 17 and 19, have bell shapes because they are directly bound to each other. Without dilution, the C-13 singlet has less than one third the intensity of the other carbons (12.6% instead of 47.6 for C-1). When considering all $J_{\text{CC}} > 1$ Hz couplings farther bow these curves (Figure S6 bottom) because of ${}^2J_{13,15}$, ${}^3J_{9,15}$ and ${}^3J_{13,22}$. The amplitudes of the singlets decreases to 1.07% and five other carbons significantly deviate from the ideal straight line. Samples produced with non-diluted ($1\text{-}^{13}\text{C}_1$, 99%) and ($2\text{-}^{13}\text{C}_1$, 99%) glucose are therefore very interesting when only the carbons listed in the entries 6,7 and 9 of Table S1 are important. In terms of cost, dilution has no effect on the carbons with linear behavior, but restores the signals of the other carbons. The choice of enrichment level should therefore be made according the sensitivity of the experiment. Higher proportions of singlet can be reached using commercially available (1, 6- C_2 , 99% 1-C, 97% 6-C) glucose, but the price being about one order of magnitude higher we did not considered this source.

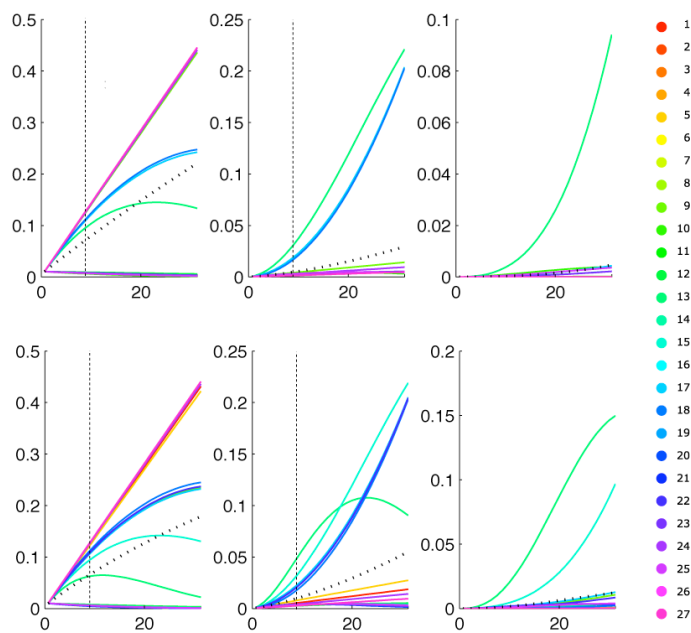


Figure S6. Simulations of the relative proportions of the carbon-13 of cholesterol obtained using (1- $^{13}\text{C}_1$, 99%) glucose (empty circles in Figure 1) as a function of the average level of ^{13}C enrichment of cholesterol. Intensities of (left) singlet (center) doublet and (right) triplet structures. Calculations took into account (top) only $^1J_{\text{CC}}$ and (bottom) all $J_{\text{CC}} > 1$ Hz.

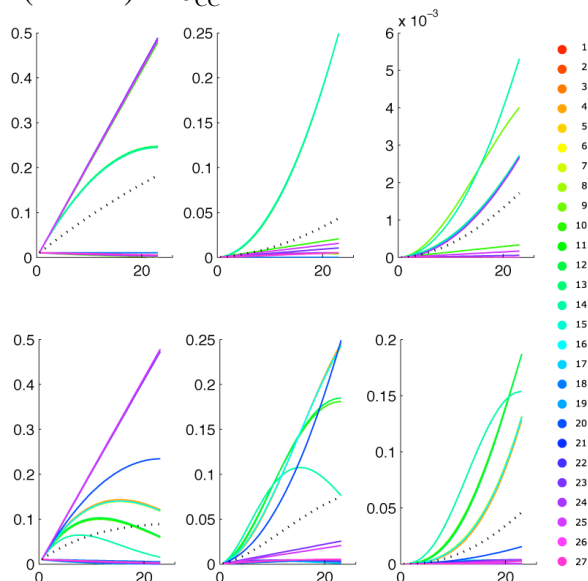


Figure S7. Simulations of the relative proportions of the carbon-13 of cholesterol obtained using (2- $^{13}\text{C}_1$, 99%) glucose (filled circles in Figure 1) as a function of the average level of ^{13}C enrichment of cholesterol. Intensities of (left) singlet (center) doublet and (right) triplet structures. Calculations took into account (top) only $^1J_{\text{CC}}$ and (bottom) all $J_{\text{CC}} > 1$ Hz.

Table S1. Table of J_{CC} coupling obtained using DFT-GIAO calculations^a

	1	2	3	4	5	6	7	8	9	10	11	12	13	14	15	16	17	18	19	20	21	22	23	24	25	26	27	J>1 ^b	J>25 ^b	
1																														
2	32																													
3		35																												
4	1	-1	37																											
5	-1	2	-1	42																										
6	2		3	3	80																									
7				4	42																									
8	2	1		4	-1	34																								
9	1	3		1	-1	4	-1	31																						
10	33	-1	1	2	39	1	2	-1	35																					
11	1			2	3	-1	35																							
12					1	3	1	-1	3	33																				
13					1	3	1	1	-1	34																				
14					3		36	-1	2	2																				
15					1		1	3		3	2	33																		
16							4			4	2	1	33																	
17							3			3	34	4	1	33																
18							1			1	1	34																		
19	1	1			-1	2	-1	1		34	2																			
20																														
21																														
22																														
23																														
24																														
25																														
26																														
27																														

^a For the geometry optimization, carbons 22-27 were removed. The couplings of the latter carbons have been introduced manually according to the values expected for a mobile side chain.

^b Number of coupling larger than 1 and 25 Hz respectively.